Majority-carrier capture cross-section determination in the large deep-trap concentration cases

J. R. Morante, J. Samitier, A. Cornet, A. Herms, and P. Cartujo
Càtedra d'Electrònica, Facultat de Física, Universitat de Barcelona, Spain

(Received 6 August 1985; accepted for publication 31 October 1985)

A method to determine the thermal cross section of a deep level from capacitance measurements is reported. The results enable us to explain the nonexponential behavior of the capacitance versus capture time when the trap concentration is not negligible with respect to that of the shallow one, and the Debye tail effects are taken into account. A figure of merit for the nonexponential behavior of the capture process is shown and discussed for different situations of doping and applied bias. We have also considered the influence of the position of the trap level's energy on the nonexponentiality of the capture transient. The experimental results are given for the gold acceptor level in silicon and for the *DX* center in $Al_{0.55}Ga_{0.45}As$, which are in good agreement with the developed theory.

I. INTRODUCTION

The measurements of the thermal cross section and its dependence on temperature are essential to obtain a thorough picture of the deep levels. While the indirect measurements are immediately rejected due to their lack of precision, the direct methods are more reliable when the deep-trap-to-shallow-concentration ratio N_T/N is small and the influence of the edge region is negligible.

However, in most cases these conditions do not hold. When the edge-region influence is not negligible, the capture probability is nonuniform. The existence of the free-carrier tail extending from the bulk towards the junction establishes two regions of capture, fast and slow, which pose problems in the interpretation of the results. So, after each pulsed bias the transient will have two components. Several authors have dealt with this problem. However, only the $N_T/N < 0.1$ case has generally been considered.[1-7] Recently, some initial models have also been carried out for the large deep-trap-to-donor-concentration ratio,[8,9] in which case the fast component also presents a nonexponential behavior, which becomes more important as the N_T/N ratio increases.

In the present work, we analyze the effects of a high N_T/N ratio and deduce a method for the suitable interpretation of the usual semilogarithm plot of the capacitance variation versus the capture time. We have taken into account that the capture process is originated as in the neutral semiconductor as in the Debye tail. Besides the dependence of the capacitance with regard to the junction bias, concentration ratio, and the applied bias pulse for different capture time, it has also been analyzed and expressed using a figure of merit. The experimental values obtained for the gold acceptor level in silicon are in good agreement with the developed model, which has also been applied to deduce the electron capture cross section of the *DX* center in $Al_{0.55}Ga_{0.45}As$. Its behavior concurs with the conclusions deduced from this model.

II. ANALYSIS

We assumed that the semiconductor contains a constant volume density N_D of shallow donors and a density N_T of a donor deep level with a free ionization energy E_T which lies below the Fermi level E_F in the bulk. The band diagrams of an *n*-type Schottky barrier in the sequence of events during the measurement are shown in Fig. 1.

Let $W_2(0)$ be the depletion width and $W_{2\lambda}(0)$ the crossover position of the Fermi level and the trap level in its steady state with an applied bias V_2 [Fig. 1(a)]. When a bias pulse of height V_1-V_2 is applied, the depleted region width shrinks initially to W_1 and those centers between W_1 and $W_{2\lambda}(0)$ begin to capture electrons [Fig. 1(b)]. Moreover,

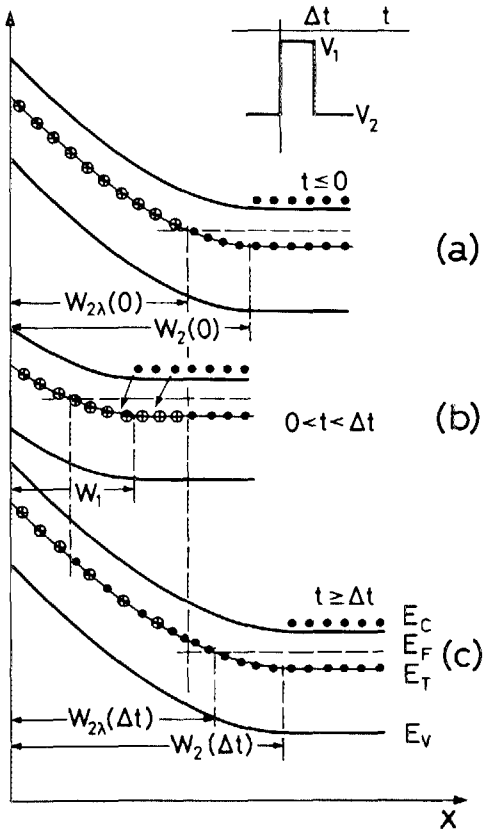

FIG. 1. Band diagrams at different time sequences: (a) Steady-state condition at V_2 bias. (b) Capture condition when a V_1-V_2 bias pulse is applied. (c) Emission condition when the bias pulse is removed.

 0021-8979/86/051562-08$02.40

some levels will also be filled in the region between $W_{1\lambda}(\Delta t)$ and $W_1(\Delta t)$ due to the Debye tail of the bulk electrons during the pulse time Δt. The width of this region $W_{1\lambda} - W_1 = \lambda_1$ can be deduced by assuming that the occupancy factor at $W_{1\lambda}$ is half of the value of $f_N(\Delta t)$, obtained in the neutral region which was given in a previous work;[9] we take into account that the free-carrier concentration changes to keep the charge neutrality out of the space-charge layer.

$$f_N(\Delta t) = \frac{n_T(\Delta t)}{N_T^*} = \frac{(N_T^*/N_T)(1 - e^{-\eta \Delta t})}{1 - (N_T^*/N_D^*)e^{-\eta \Delta t}}, \quad (1)$$

where

$$N_T^* = N_T \frac{2(N_D + N_T)}{N_D\left[\sqrt{1 + 2\gamma\epsilon + \gamma^2} + (\epsilon + \gamma)\right]}, \quad (2)$$

$$N_D^* = N_T \frac{-2(N_D + N_T)}{N_D\left[\sqrt{1 + 2\gamma\epsilon + \gamma^2} - (\epsilon + \gamma)\right]}, \quad (3)$$

$$\gamma = e_n/c_n N_D, \quad (4)$$

$$\epsilon = (N_D + 2N_T)/N_D, \quad (5)$$

$$c_n N_D = \eta\left[\sqrt{1 + (e_n^2/2)(\epsilon^2 - 1)} - (e_n/\eta)\epsilon\right], \quad (6)$$

and e_n and c_n are, respectively, the emission and capture thermal coefficients. In our experimental case $e_n \ll c_n N_D$, thus the above expressions can be approximated by

$$f_N(\Delta t) = \frac{n_T(\Delta t)}{N_T} = \frac{1 - e^{-\eta \Delta t}}{1 - [N_T/(N_D + N_T)]e^{-\eta \Delta t}}, \quad (7)$$

where

$$\eta = c_n N_D = \sigma_n \langle v \rangle N_D. \quad (8)$$

In order to obtain the time evolution of the edge region from these assumptions, it is necessary to solve the detailed balance equations in the edge region with the corresponding boundary conditions given by Eq. (7):

$$\frac{df(x,\Delta t)}{dt} = c_n n(x,\Delta t)[1 - f(x,\Delta t)] - e_n f(x,\Delta t), \quad (9)$$

where $n(x,\Delta t)$ must be the exact distribution of the free carriers in this region. So we have

$$n(x,\Delta t) = \{N_D + N_T[1 - f_N(\Delta t)]\}e^{-qV(x,\Delta t)/kT}, \quad (10)$$

where $V(x,\Delta t)$ is the potential distribution in the space-charge region which is known by solving the Poisson equation:

$$\frac{\partial^2 V(x,\Delta t)}{\partial x^2} = -\frac{q}{\epsilon_s}\{N_D + N_T \times [1 - f_N(x,\Delta t)] - n(x,\Delta t)\}, \quad (11)$$

where ϵ_s is the permittivity of the semiconductor and q the electron charge.

The numerical calculation of these equations must be performed in an iterative form. For each time Δt, $n(x,\Delta t)$ and $f(x,\Delta t)$ are obtained from Eqs. (9) and (10) by assuming that $V(x,\Delta t)$ has remained momentarily equal to $V[x,\Delta t - \delta(\Delta t)]$, with $\delta(\Delta t)$ being the increment of time.

$W_1(\Delta t)$ has been deduced in accordance with the results of Warner and Jindall[10] from the position where

$$qV(W_1,\Delta t)/kT = -\ln 0.55,$$

and $\lambda_1(\Delta t)$ is given by the condition

$$f(W_1 - \lambda_1,\Delta t) = f_N(\Delta t)/2. \quad (12)$$

It should be pointed out that in the large deep-trap concentration cases, unlike the $N_T/N_D < 0.1$ case, the available free-carrier concentration to participate in the capture process at any position of the edge region changes due to the capture process in the neutral region, given by Eq. (1). At the beginning of the process the concentration of free carrier at this region is $N_T + N_D$ but becomes N_D in about five capture-time constants. So, initially, the free-carrier charge in the space-charge layer diminishes, and the edge-region capture becomes more difficult. Therefore, $\lambda_1(\Delta t)$ remains very small and can even decrease when the occupancy factor f_N increases, since the corresponding diminution of $n(x,\Delta t)$ allows condition (12) to be accomplished with smaller values of λ_1. This effect is more significant as N_T/N_D increases. When $f_N(\Delta t)$ has approached its maximum value, λ_1 begins to rise. In the large deep-trap concentration cases the charge change due to the edge-region capture is enough to force a considerable variation of the space-charge layer width W_1.

In Fig. 1(c), a band diagram after the application of the bias pulse is shown. Now $W_2(\Delta t)$ and $W_{2\lambda}(\Delta t)$ are the new values for the depletion width and the crossover point, which are functions of the values $W_1(\Delta t)$ and $\lambda_1(\Delta t)$. The decrease of the charge in the space-charge layer, due to the capture process, is balanced by an increase of the space-charge layer width $W_2(\Delta t)$. However, to obtain its value it is necessary to know $W_1(\Delta t)$ and $\lambda_1(\Delta t)$ *a priori*. It can be deduced exactly by solving the above equations for the space-charge layer biased at V_1, assuming constant profiles for N_D and N_T.

In the last years several works[6,7,11-14] have been devoted to deduce the analytical expressions of the time evolution of the edge-region width under different conditions. In the present work we used an alternative to the exact solution of Poisson's equation. It involves solving the capture kinetics equation at the edge region, assuming for each Δt a free-carrier concentration at W_1, given by the solution of the capture process in the bulk. Then we obtain a simple analytical approximation which we use elsewhere[15]:

$$[c_n n(x,\Delta t) + e_n]\Delta t = \ln\left(\frac{2}{(2 - f_N) - [e_n/c_n n(x,\Delta t)]f_N}\right). \quad (13)$$

Once n is known, the band-bending energy $qV_\lambda(\Delta t)$ corresponding to the position where $f = f_N/2$ is deduced from Eq. (13). A good approximation is given by

$$V_\lambda = \frac{kT}{q}\ln\left(\frac{c_n N_D \Delta t}{\ln\left(\frac{2}{(2 - f_N) - [e_n/c_n n(\lambda)]f_N}\right)} + 1\right). \quad (14)$$

This result is in good agreement with approximations obtained by other authors.[6,7,11-14] Now $W_1(\Delta t)$ and $\lambda_1(\Delta t)$ can be calculated, assuming that the trap occupancy is zero for $x < W_1 - \lambda_1$ and $f_N(\Delta t)$ for $W_1 - \lambda_1 < x < W_1$. So, we obtain

$$W_1(\Delta t) = \Big\{ (N_T/N_D) f_N \lambda_1 + \sqrt{2L_D^2(1+N_T/N_D)\{[q(V_1+V_B)/kT]-1\} - (N_T/N_D) f_N \lambda_1^2 + [(N_T/N_D)\lambda_1]^2 (f_N^2 - f_N)} \Big\} \times (1+N_T/N_D)^{-1}, \quad (15)$$

and

$$\lambda_1(\Delta t) \simeq \sqrt{2}\, L_D \sqrt{(qV_\lambda/kT) - f_N}\,, \quad (16)$$

where V_B is the built-in potential and

$$L_D = \sqrt{\epsilon_s\, kT/q^2 N_D}\,. \quad (17)$$

Figures 2 and 3 show, respectively, the variation of λ_1 and W_1 versus the capture time computed for the gold acceptor level in n-Si at 80 K for different N_T/N_D ratios, with $\sigma_n = 7\times10^{-17}$ cm^2, $N_D = 1.35\times10^{14}$ cm^{-3}, and $V_1 = 0$.

It should be pointed out that the calculated λ_1 values behave as we had previously predicted. W_1 is initially constant. It increases due to the variation of the fraction of occupied traps; afterwards, the changes are only produced by the λ_1 variation. The total variation of W_1 is approximately 1 order of magnitude smaller than its initial value, for $N_T/N_D < 0.1$; but when N_T/N_D increases toward unity, the variation of W_1 is comparable to its initial value. Obviously, this considerable rearrangement of the space-charge layer at V_1 determines the new value of the space-charge layer when the bias is returned to V_2.

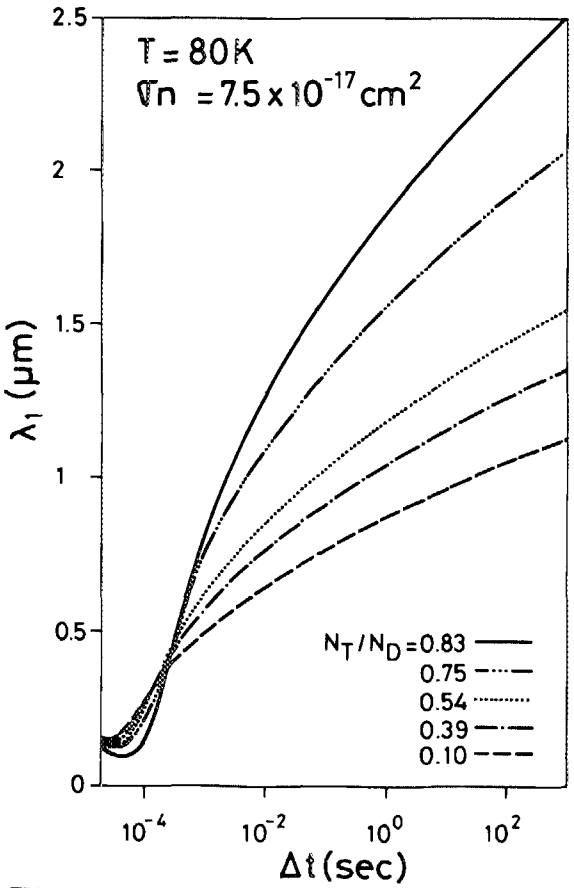

FIG. 2. Edge region width λ_1 vs the capture time calculated for the gold acceptor level in p^+n silicon diode at 80 K and $V_1 = 0$. Values used are $\sigma_n = 7.5\times10^{-17}$ cm^{+2} and $N_D = 1.35\times10^{14}$ cm^{-3} for different N_T/N_D ratios.

Since the bias V_2 is fixed, we have at any time

$$|V_2 + V_B| = 1/\epsilon_s \int_0^1 x\rho(x,\Delta t + t)dx\,, \quad (18)$$

where

$$\rho(x,\Delta t + t) = q\{N_D - n(x,\Delta t + t) + N_T[1 - f(x,\Delta t + t)]\}\,. \quad (19)$$

$n(x,\Delta t + t)$ and $f(x,\Delta t + t)$ are, respectively, the values of the free-majority carriers and occupancy factor at the x position after being biased during t seconds at V_2; "1" is any point in the neutral region.

To eliminate the effects due to the emission of the trapped charge we consider only the initial value for $t = 0$; hence, the f value in the above expression corresponds to the final value of the occupancy factor during the capture process. Like the above case for V_1, Eq. (18) can only be solved by a long computer process.

In order to deduce useful solutions for Eq. (18), we have assumed similar approximations to the $N_T \ll N_D$ case.[6] Thus, we have considered that the filling of the traps happens in the region between $W_{1\lambda}(\Delta t)$ and $W_{2\lambda}(0)$ and that its occupancy factor becomes $f(\Delta t)$. This is equivalent to saying that we replace the true occupancy factor with a new rectangular occupancy factor f_R defined by

$$f_R = 0, \quad x < W_{1\lambda}\,,$$
$$f_R = f_N(\Delta t), \quad W_{1\lambda} < x < W_{2\lambda}(0)\,,$$

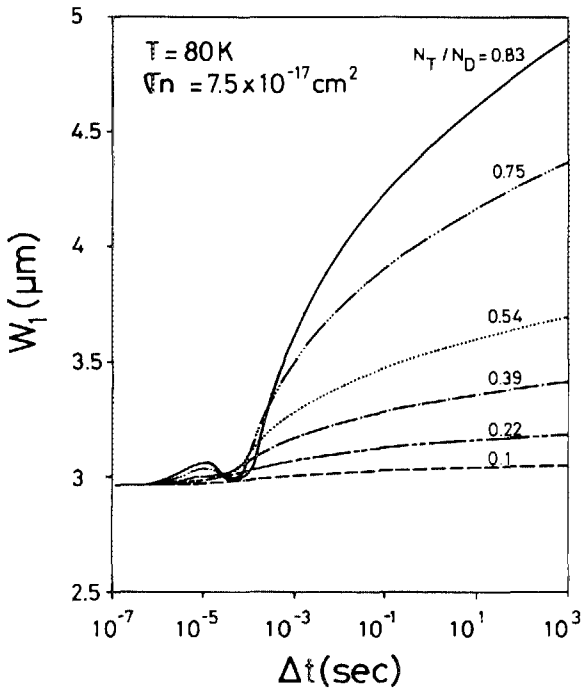

FIG. 3. Space-charge layer width vs the capture time at the same conditions of Fig. 2.

and

$$f_R = f_N(\infty), \quad W_{2\lambda}(0) < x .$$

We consider that the fast decrease of the free-carrier density at the edge region occurs like the small deep-trap concentration case. Therefore, the approximation of a rectangular occupancy factor has validity as in the small deep-trap concentration case. So, expression (18) can be approximated by

$$\frac{\epsilon_s}{q}(V_2 + V_B) = \int_0^{W_1(\Delta t)} (N_D + N_T)x dx + \int_{W_{1\lambda}(\Delta t)}^{W_{2\lambda}(0)} [N_D + N_T - n_T(x,\Delta t)]x dx + \int_{W_{2\lambda}(0)}^{W_2(\Delta t)} [N_D - n(x,\Delta t)]x dx . \quad (20)$$

In spite of the fact that we do not use the depletion approximation, the high-frequency capacitance $C_{HF} = \epsilon_s A/W$ remains rigorous, so that it can be checked by calculating directly $C = dQ/dV$ at high frequency. Then, making straightforward calculations we obtain

$$\frac{dC_2}{d(\Delta t)} = -\eta e^{-\eta\Delta t}\left(\{N_T/[2(N_D+N_T)]\}\left(\frac{1}{1 - N_T/(N_D+N_T)e^{-\eta\Delta t}}\right)^2 \times\left[\left(1-\frac{\lambda_0}{W_2(0)}\right)^2 \frac{C_2^3(\Delta t)}{C_2^2(0)} - \left(1-\frac{\lambda_1(\Delta t)}{W_1(\Delta t)}\right)^2 \frac{C_2^3(\Delta t)}{C_1^2(\Delta t)}\right]\right), \quad (21)$$

where $\lambda_0 = W_2(0) - W_{2\lambda}(0)$. This parameter has been deduced from the exact integration of Poisson's equation at equilibrium:

$$\lambda_0 = \sqrt{[2\epsilon_s(E_F - E_T)/q^2 N_D] - (2\epsilon_s kT/q^2 N_D)} , \quad (22)$$

where $E_F - E_T$ is the energetic separation between the majority carrier's quasi-Fermi level and the trap level.

Due to the complexity of Eq. (21), we have solved it taking into account three time intervals.

(a) For short capture times, we obtain

$$-\frac{\eta}{N_D} = -c_n = \frac{N_D}{N_T}\frac{2}{N_D+N_T}\frac{W_2^3(0)}{W_{2\lambda}^2(0) - W_{1\lambda}^2} \times\frac{1}{\epsilon_s A}\frac{dC_2}{d(\Delta t)}\bigg|_{\Delta t\to 0}, \quad (23)$$

where A is the area. In this case, the denominator imposes a restrictive condition $W_{2\lambda}(0) > W_{1\lambda}$, which yields

$$\frac{V_1 - V_2}{V_2} \geq 1 - \left(1 - \frac{\lambda_0}{W_2(0)} + \frac{\lambda_1(\Delta t)}{W_2(0)}\right)^2 . \quad (24)$$

On the other hand, one observes that $dC_2/d\Delta t\,|_{\Delta t\to 0}$ depends on the polarization through $W_2^3(0)/(W_{2\lambda}^2 - W_{1\lambda}^2)$ and on the doping. Moreover, when the above restrictive condition is fulfilled $dC_2/d\Delta t\,|_{\Delta t\to 0}$ is greater or equal to η. This will be analyzed below when we present the figure of merit.

(b) For greater capture times in expression (21), the exponential variation versus time is stronger than that of the term in bracket. It is due to the logarithmic dependence of λ_1 on Δt. So, we can write

$$C_2(\Delta t) - C_2(\infty) = M(\Delta t)e^{-\eta\Delta t}, \quad (25)$$

where

$$M(\Delta t) = \frac{N_T}{2(N_D+N_T)}\left(\frac{1}{1 - N_T/(N_D+N_T)e^{-\eta\Delta t}}\right)^2 \times\left[\left(1-\frac{\lambda_0}{W_2(0)}\right)^2 \frac{C_2^3}{C_2^2(0)} - \left(1-\frac{\lambda_1}{W_1}\right)^2 \frac{C_2^3}{C_1^2}\right]. \quad (26)$$

Now the slope of the semilogarithmic plot of $C_2(\Delta t) - C_2(\infty)$ vs Δt changes continually from the initial values towards lower ones. However, when $M(\Delta t)$ depends slightly on Δt, the semilogarithmic plot shows a region, whose slope is near to η.

(c) Further capture-time increases give rise to a lower dependence of $dC_2/d\Delta t$ in relation to Δt due to greater λ_1 influence. This, every time, increases more slowly due to the fact that the free-carrier concentration falls when λ_1 increases. It gives rise to a very soft variation of the capacitance which makes it hard to obtain the saturation capture values corresponding to $\lambda_1 = \lambda_0$.[6,7] This process becomes slower as the level is deeper.

III. RESULTS AND DISCUSSION

From the above analysis we can deduce important aspects in relation to the fitting between the experimental data and the theoretical values of $C_2(\Delta t)$.

The calculated capacitance variation in the final part of the transient shows a great dependence on the energy position of the level, through the λ_1 values, as can be seen in Fig. 4. This dependence makes it very difficult to use this part of the capture transient to determine the capture cross section if the energy position is not well known.[6]

On the contrary, the initial part of the capture transient depends more on the doping conditions and on the capture cross section than on the energy position; but the dependence on the concentration is so strong that it is not very easy to determine the capture cross section by the fitting of the experimental capacitance variation, unless the N_T/N_D ratio is known with high accuracy (Fig. 5). Accordingly, we have taken great care over the determination of the energy position of the level and the concentration values in order to obtain a whole fitting of the capture transient with our model.

The experimental study has been carried out on the *DX* donor center in n-$Al_{0.55}Ga_{0.45}As(Te)/p$-$Al_{0.35}Ga_{0.65}As(Ge)$ heterojunction and on the gold acceptor level in P^+N silicon diodes. More details of the samples are given elsewhere.[9,11] Capacitance isothermal transients have been

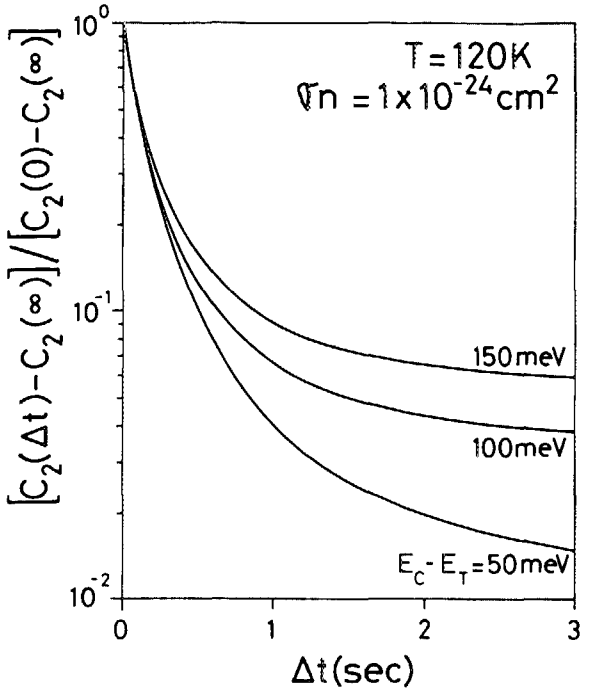

FIG. 4. Theoretical capacitance change vs capture time for a donor level for different energy positions in an $Al_xGa_{1-x}As$ heterojunction, with $x = 0.55$. The values used are $\sigma_n = 1\times10^{-24}$ cm^2, $T = 120$ K, $N_D = 1.2\times10^{17}$ cm^{-3}, and $N_T = 1.75\times10^{17}$ cm^{-3}.

recorded, using a Boonton model 72BD monitored by a computer. The bias pulses have been applied using a HP 8013A and a HP 214A.

For the $Al_xGa_{1-x}As$ heterojunctions we have determined $N_D = 1.2\times10^{17}$ cm^{-3} and $N_T = 1.75\times10^{17}$ cm^{-3} from $C(V)$ measurements. At each voltage, the capacitance values for $\Delta t = 0$ and $\Delta t = \infty$, corresponding to zero and the maximum electron occupancy factor, have been measured, respectively, by lowering slowly the temperature (from a high enough value for the thermal emission to take place) with the bias applied or with the sample in short circuit and by applying the reverse bias required when the low temperature has been reached. Thus, we have the situation discussed above for C_2 and C_1 in the $\Delta t = 0$ and $\Delta t = \infty$ conditions.

Figure 6 shows the capacitance transients for the heterojunction at different V_1 values at 77 K. Their behavior corroborates the above theoretical results described. They are nonexponential even though the bias variation is small; in this case, however, the capture happens only at the edge region, since condition (24) is not fulfilled. For greater bias pulses $V_1 = 0$ and $V_2 = 5$ V, the above condition is fulfilled and the initial decays are faster according to condition (23).

Figure 7 shows the semilogarithmic plot of the capacitance variation versus t at different temperatures for the DX center. The continuous lines indicate the results of our model, which give us the same values for C_2 as the exact computer calculation of Poisson's equation [Eq. (18)]. This justifies the use of the equations deduced to determine C_2. The dots correspond to our experimental measurements. In this case, at each temperature the experimental data have been fitted using different values of σ_n. Figure 8 shows the Arrhenius plot of the best values of σ_n vs $1000/T$. The slope corresponds to an electron cross section activated with the temperature according to

$$\sigma_n = 1.5\times10^{-19}\exp-(125/kT)\,. \tag{27}$$

So, the activation energy of the capture process is $E_a = 125$ meV.

We have used an energy position $E_T = 35$ meV, which is in good agreement with $E_a + E_T$ deduced elsewhere[15] from

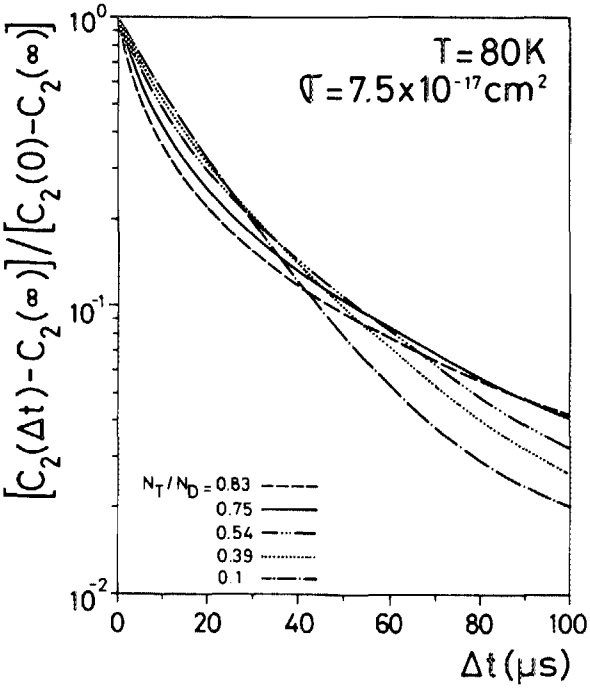

FIG. 5. Theoretical capacitance change vs capture time for an acceptor level for different N_T/N_D ratios in a silicon p^+n junction. The values used are $\sigma_n = 7.5\times10^{-17}$ cm^2, $E_T = 548$ meV, $T = 80$ K, and $N_D = 1.35\times10^{14}$ cm^{-3}.

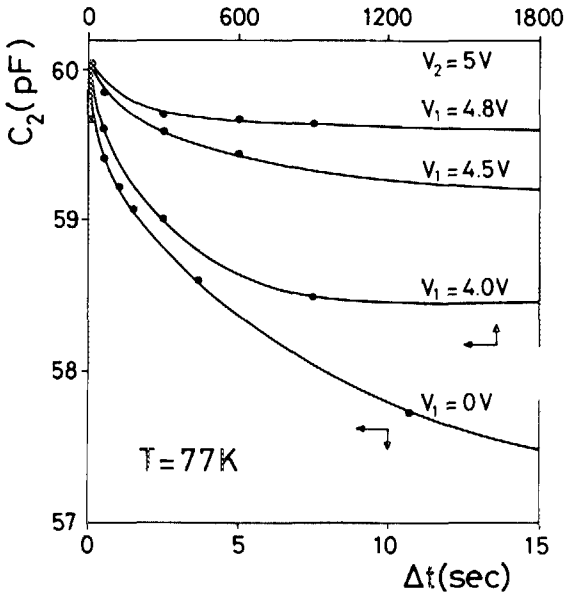

FIG. 6. Capacitance vs the capture time measured on the DX center in n-$Al_{0.55}Ga_{0.45}As$: p-$Al_{0.35}Ga_{0.65}As$ heterojunction at 77 K for different bias condition. $N_D = 1.2\times10^{17}$ cm^{-3}; $N_T = 1.45N_D$.

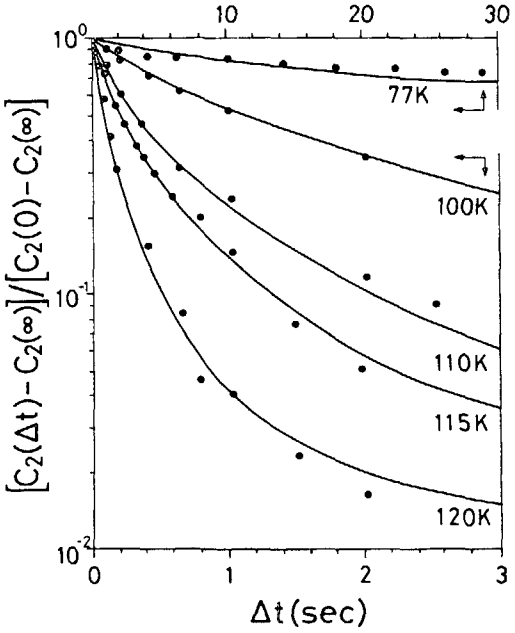

FIG. 7. Semilogarithmic plot of the capacitance variation vs the capture time at different temperatures for the *DX* center. The continuous lines indicate the theoretical results according to our model with $E_T = 35$ meV. The dots correspond to experimental measurements. The concentration data are the same in Fig. 6.

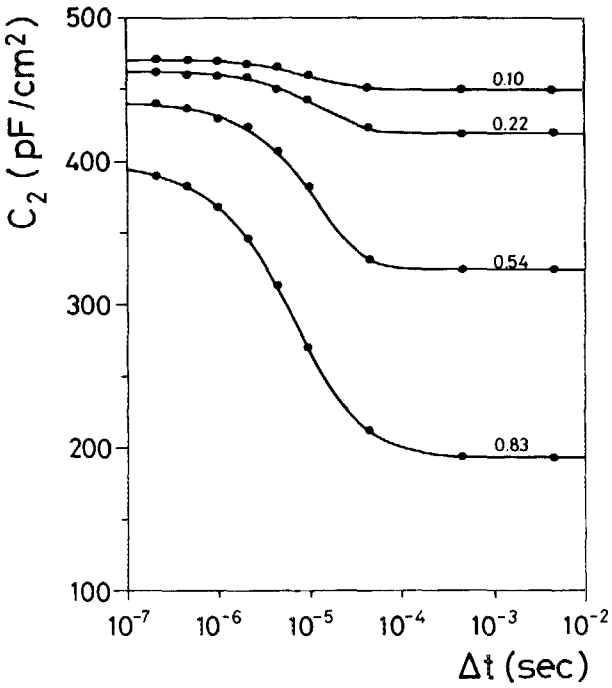

FIG. 9. Theoretical capacitance at V_2 vs the capture time at 80 K for the gold acceptor level in a p^+n silicon diode at different N_T/N_D values. The dots indicate the experimental results. $N_D = 1.35\times10^{14}$ cm^{-3} and $\sigma_n = 7.5\times10^{-17}$ cm^2.

the Arrhenius plot of the emission coefficient (160 ± 5 meV). Moreover, it agrees with the energy position given by other authors[16]. If we use a greater value of E_T, a relatively good fitting can still be obtained, but there is no self-consistency with emission results.

Figure 9 shows C_2 vs Δt for the gold acceptor level at 80 K and different N_T/N_D values. Unlike the *DX* center, the thermal cross section of the gold acceptor level does not show dependence with the temperature. In this case the energy position of the level is well known. Therefore, the fitting is easier. The best value of σ_n to fit each measurement turns out to be independent of the N_T/N_D ratio in good agreement with our previous work,[9] and so confirms the developed analysis. The value deduced is

$$\sigma_n = 7.5\times10^{-17}\ \text{cm}^{+2}.$$

Figure 10 shows the semilogarithmic plot of the capacitance variation versus Δt for $N_T/N_D = 0.75$ and 0.1. In the last case the nonexponential behavior is only denoted at long time intervals, while, in the other case, it is observed in the whole transient.

In order to know, *a priori*, how nonexponential the capture transient is, we have defined a figure of merit by the ratio between the time constant deduced from the initial part of the transient, supposing the single exponential model η^* and the true value η,

$$\eta^* = \frac{1}{C_2(0) - C_2(\infty)} \frac{dC_2}{d(\Delta t)}\bigg|_{\Delta t\to 0}. \tag{28}$$

It provides us with information regarding the inaccuracy of the exponential model:

$$R = \frac{\eta^*}{\eta} = \frac{N_T}{N_D}\left(1+\frac{N_T}{N_D}\right) \times \frac{(r-s_0)^2-(u-s_1)^2}{2r^2(1-r)}, \tag{29}$$

where the nonindependent variables r, s_0, s_1, and u are, respectively, $W_2(0)$, $W_2(0) - W_{2\lambda}$, $W_1 - W_{1\lambda}$, and W_1 nor-

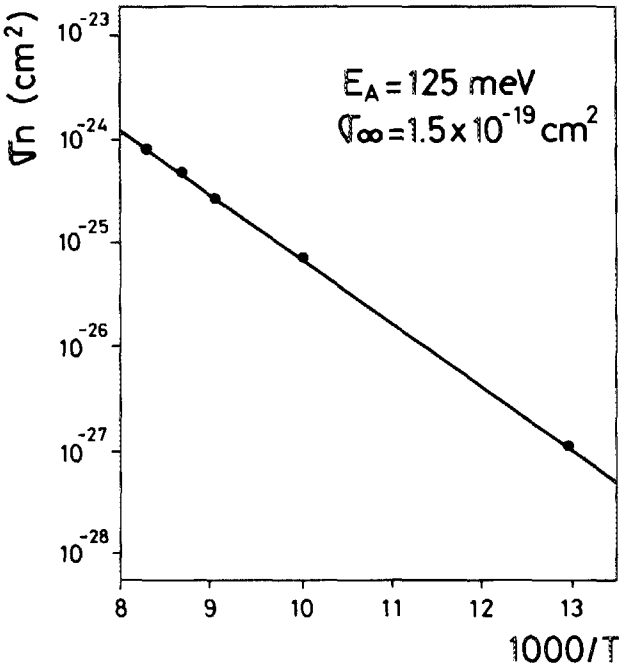

FIG. 8. Arrhenius plot of the electron cross-section values obtained for the *DX* center from the fitting shown in the former figure.

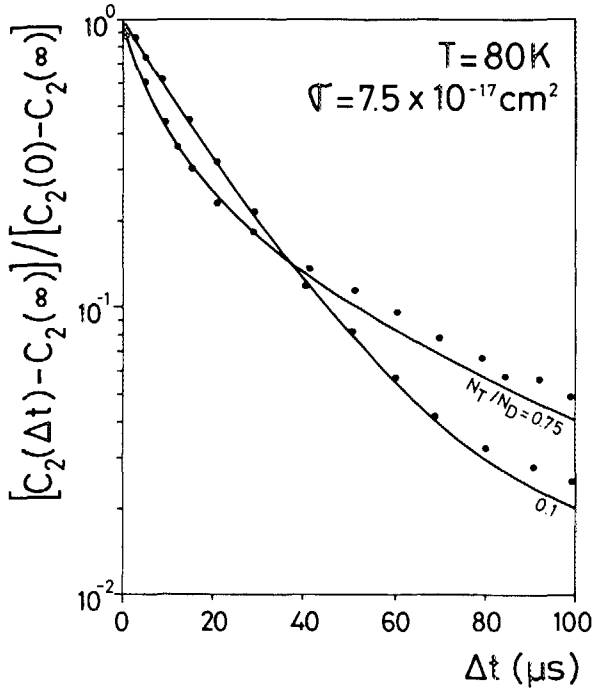

FIG. 10. Theoretical semilogarithmic plot of the capacitance variation vs the capture time for the gold acceptor level in a silicon p^+n junction at 80 K for $N_T/N_D = 0.75$ and 0.1. The data are the same as in the former figure. The dots are the experimental values.

malized to $W_2(\infty)$. Figure 11 shows the theoretical plot of R vs u, using the N_T/N_D values as a parameter. We observe that if condition (24) is fulfilled, we have:

(a) R is always greater than one, when N_T/N_D is not negligible. It should be pointed out that the condition

$$N_T[(r-s_0)^2-(u-s_1)^2] = N_D(1-r^2)$$

must be always fulfilled.

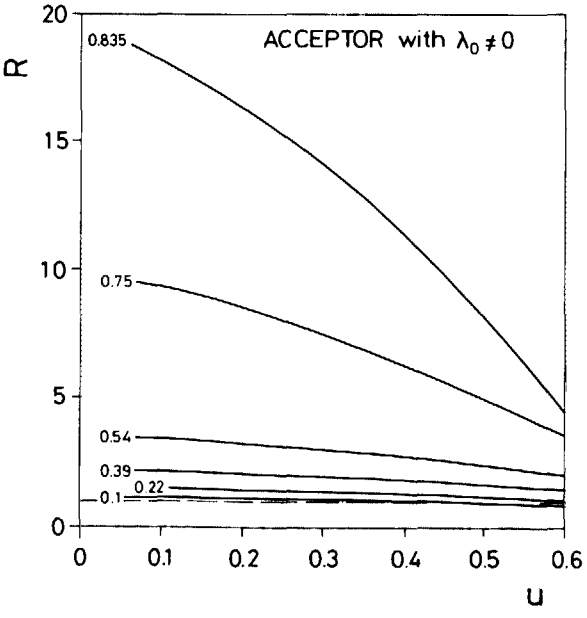

FIG. 11. Computer data of the nonexponential figure of merit R for the gold acceptor level in silicon p^+n junction at several values of N_T/N_D, with the data of the former figure.

(b) R increases as N_T/N_D is raised, which indicates the important effects of the large deep-trap concentration case on the nonexponentiality of the capacitance capture transients.

(c) $R \to 1$ as $N_T/N_D \to 0$. However, if inequality (24) is not fully accomplished, R can be smaller than 1, since in this case the predominant region where the capture happens is the edge region.

(d) When V_1 approaches V_2, the nonexponential behavior remains in spite of the small variation of the bias. If we consider that the effects of large N_T become more important than those of the edge region, when $\lambda_0 \to 0$, the figure of merit R can be extrapolated to $1 + N_T/N_D$. It indicates that to obtain an exponential capture transient it is more significant to have a small trap density than to apply small bias pulses.

(e) For fixed N_T/N_D, R increases as u is decreased, which corroborates the strong influence of N_T/N_D and the applied bias on the capture transient form.

(f) The computer estimation of the error made on R, using approximation (8) to solve Eq. (6) always gives a value lower than 7% in the worst case.

This analysis holds for the acceptor level by replacing N_D by $N_D - N_T$.

IV. CONCLUSIONS

To summarize, we have analyzed the capacitance variation versus capture time, and we have explained its behavior in the large deep-trap concentration case. Large values of N_T/N_D give rise to a strong modification of the capture transient. First, there appears a considerable increase of the slope of the logarithm of the capacitance variation versus the capture time. Afterwards, the effects of the edge region are the determining factors that produce the nonexponential behavior. These effects are enhanced for large deep-trap concentration if the level is deeper. However, if inequality (24) is not fulfilled, the edge region always determines the slope. So, in agreement with the results of Wang and Sah[17] for the emission transients, the only guarantee for an exponential transient is a small concentration ratio, $N_T/N_D < 0.1$.

The corresponding theoretical equations for free carrier's capture by deep-level impurities in the space-charge layer and in the neutral region have also been calculated. For this capture an analytical approximation for the edge-region width has been given. Due to its logarithmic dependence on the capture time one should note that at low temperature when the pulse bias is applied, thermal equilibrium is not reached, although the capacitance variations show a fixed value.[18,19] The N_T/N_D ratio has been found to have great influence on the λ_1 determination and on the W_1 variation. Therefore, we have taken special care in the concentration values determination from the C-V measurements.

The developed model provides a method to measure the thermal cross section from an easy numerical simulation of the semilogarithmic plot of the capacitance variation versus Δt. The experimental results found for the electron cross section of the well-known gold acceptor level in p^+n silicon diode agrees with that measured previously by means of other techniques,[1,2,8,9] which corroborates the developed model. Moreover, the experimental values for the DX center show a

behavior corresponding to that deduced from our model. We have found for this center that the values used in the fitting follow a law:

$$\sigma_n = \sigma_\infty \exp(-E_a/kT),$$

with $\sigma_\infty = 1.5\times10^{-19}$ cm^2 and $E_a = 125$ meV. This value agrees with the results $E_T = 35$ meV obtained from the fitting and with the activation energy deduced from the Arrhenius plot of the emission coefficients (160 ± 5 meV): $E_a = 160$–35 meV.

On the other hand, we have proposed a figure of merit in order to have a criterion to give us a measurement of the nonexponentiality of the capture transient under given conditions. The nonexponential behavior depends strongly on the N_T/N_D ratio, on the bias conditions, and on the energy position of the level through λ_1. One can see that the transient is only exponential (figure of merit equal to 1) if $N_T \ll N_D$.

Finally, it should be noted that using the constant capacitance technique also presents problems of nonexponentiality. According to expression (1), the capture in the neutral region will be nonexponential. Moreover, according to expression (15), the charge variation at the edge region will give rise to nonexponential changes of the applied bias in order to maintain the capacitance at a constant rate. However, in this case, the relation between the voltage changes and the charge variation is a little more simple than in the constant voltage case, but its experimental setup is more complex. Generally, its utilization does not present any significant advantage.

ACKNOWLEDGMENT

This work has been supported by CIRIT and CAICYT (project No. 2340/82).

[1] J. Barbolla, M. Pugnet, J. C. Brabant, and M. Brousseau, Phys. Status Solidi (A) **36**, 495 (1976).
[2] S. D. Brotherton and J. Bicknell, J. Appl. Phys. **49**, 667 (1978).
[3] A. Zilberstejn, Appl. Phys. Lett. **33**, 200 (1978).
[4] D. Pons, Appl. Phys. Lett. **37**, 423 (1980).
[5] J. M. Noras and H. R. Szawelska, J. Phys. C **15**, 2001 (1982).
[6] D. Stievenard, J. C. Bourgoin, and M. Lannoo, J. Appl. Phys. **55**, 1477 (1984).
[7] E. Meijer, H. G. Grimmeiss, and L. A. Ledebo, J. Appl. Phys. **55**, 4266 (1984).
[8] J. A. Borsuk and R. M. Swanson, J. Appl. Phys. **52**, 6704 (1981).
[9] J. R. Morante, J. E. Carceller, A. Herms, P. Cartujo, and J. Barbolla, Appl. Phys. Lett. **41**, 656 (1982).
[10] R. M. Warner and R. P. Jindal, Solid State Electron. **26**, 335 (1983).
[11] S. D. Brotherton, Solid State Electron. **26**, 987 (1983).
[12] J. M. Noras, J. Phys. C **14**, 2341 (1981).
[13] G. P. Li and K. L. Wang, Solid State Electron. **26**, 825 (1983).
[14] D. Pons, J. Appl. Phys. **55**, 3644 (1984).
[15] J. R. Morante, J. Samitier, A. Herms, A. Cornet, and P. Cartujo, Solid State Electron. (in press).
[16] J. Klem, W. T. Masselink, D. Arnold, R. Fischer, T. J. Drummond, H Morkoç, K. Lee, and M. S. Shur., J. Appl. Phys. **54**, 5214 (1983).
[17] A. C. Wang and C. T. Sah, J. Appl. Phys. **55**, 565 (1984).
[18] H. G. Grimmeiss, L. A. Ledebo, and E. Meijer, Appl. Phys. Lett. **36**, 307 (1980).
[19] A. Majerfeld and P. K. Bhattacharya, Appl. Phys. Lett. **33**, 259 (1978).